Enamel hypoplasia on rhinocerotoid teeth: Does CT-scan imaging detect the defects better than the naked eye?

Manon Hullot, Pierre-Olivier Antoine

PALÆO VERTEBRATA

ARTICLE

Enamel hypoplasia on rhinocerotoid teeth: Does micro-CT scan imaging detect the defects better than the naked eye?

Manon HULLOT* & Pierre-Olivier ANTOINE

Institut des Sciences de l'Évolution, UMR5554, Université de Montpellier, CNRS, IRD, EPHE, Place Eugène Bataillon, CC064, 34095 Montpellier, France

**corresponding author: manon.hullot@gmail.com*

Abstract: Micro-CT imaging is an increasingly popular method in paleontology giving access to internal structures with a high resolution and without destroying precious specimens. However, its potential for the study of hypoplasia defects has only recently been investigated. Here, we propose a preliminary study to test whether hypoplastic defects can be detected with micro-CT (µCT) scan and we assess the costs and benefits of using this method instead of naked eye. To do so, we studied 13 fossil rhinocerotid teeth bearing hypoplasia from Béon 1 (late early Miocene, Southwestern France) as positive control and 11 teeth of the amynodontid *Cadurcotherium* (Oligocene, Phosphorites du Quercy, Southwestern France), for which enamel was partly or totally obscured by cement. We showed that all macroscopically-spotted defects were retrieved on 3D reconstructions and selected virtual slices. We also detected additional defects using µCT scan compared to naked eye identification. The number of defects detected using µCT was greater in the *Cadurcotherium* dataset (paired-sample Wilcoxon test, p-value = 0.02724) but not for our control sample (paired-sample Wilcoxon test, p-value = 0.1171). Moreover, it allowed for measuring width and depth of the defects on virtual slices (sometimes linked to stress duration and severity, respectively), which we could not do macroscopically. As µCT imaging is both expensive and time consuming while not drastically improving the results, we recommend a moderate and thoughtful use of this method for hypoplasia investigations, restricted for instance to teeth for which enamel surface is obscured (presence of cement, uncomplete preparation, or unerupted germs).

Keywords: rhinocerotoids, fossil teeth, micro-CT imaging, method

Submitted 6 July 2021, Accepted 17 November 2021
Published Online 03 January 2022, doi: 10.18563/pv.45.1.e2

INTRODUCTION

Hypoplasia is a common defect of the enamel and, although non-specific in its etiology, a permanent and sensitive individual marker of stress (Neiburger, 1990; Guatelli-Steinberg, 2001). It is caused by a stop during enamel deposition (i.e., amelogenesis) due to a stress or a combination of stresses (Goodman & Rose, 1990). Enamel hypoplasia has been widely studied in primates and especially in humans (Ogilvie *et al*., 1989; Goodman & Rose, 1990; Lukacs, 1999; Franco *et al*., 2007; Skinner & Pruetz, 2012; Cabec *et al*., 2015; McGrath *et al*., 2018), but it has been reported and investigated in many other mammal groups (pigs: Dobney & Ervynck, 2000; sheep and goats: Kierdorf *et al*., 2012; Upex & Dobney, 2012; giraffes: Franz-Odendaal *et al*., 2004; bisons: Niven *et al*., 2004; rhinoceros: Bratlund, 1999; Mead, 1999; Fourvel *et al*., 2015; Bacon *et al*., 2018). More than a hundred causes have been proposed in humans (Small & Murray, 1978), but the most commonly proposed in the literature are: nutritional stress (Goodman & Rose, 1991; Barrón-Ortiz *et al*., 2019), seasonality (Franz-Odendaal *et al*., 2003; Skinner & Pruetz, 2012; Upex & Dobney, 2012), weaning or cow-calf separation (Goodman & Rose, 1990; Mead, 1999; Dobney & Ervynck, 2000), birth (Mead, 1999; Niven *et al*., 2004; Upex & Dobney, 2012), and diseases (Bratlund, 1999; Rothschild *et al*., 2001).

Despite this abundance of studies, no consensus concerning the method of study has been reached making cross-comparisons complex (Hassett, 2014). For instance, the identification of defects remains an issue, as no threshold has been proposed to differentiate between "normal" and pathological enamel, and as their manifestation on teeth is species-, tooth-, and individual-dependent (Neiburger, 1990; McGrath *et al*., 2021). The most commonly used approach is naked eye, sometimes coupled with hand-lens (5x or 10x), and it consists in spotting the defects, categorizing them (e.g., pit, linear), and caliper measurements (Ensor & Irish, 1995; Dobney & Ervynck, 1998; Franz-Odendaal *et al*., 2004; Niven *et al*., 2004; Fourvel *et al*., 2015; Bacon *et al*., 2018, 2020). Some studies have also used microscopy (optic, SEM, or confocal) to investigate enamel hypoplasia, either through histology (Rose, 1977; Witzel *et al*., 2008; Sabel *et al*., 2010; Marchewka *et al*., 2014), or at the surface of the enamel (directly or on casts; Chollet & Teaford, 2010; Hassett, 2014; Henriquez & Oxenham, 2017; McGrath *et al*., 2018). Microscopy allows for a better individual age estimation as Retzius lines or perikymata might be visible, but the histology approach is destructive as it requires to slice the specimen.

More recently, micro-CT scan (µCT scan) imaging has been used to study hypoplasia (Windley *et al*., 2009; Marchewka *et al*., 2014; Xing *et al*., 2016). Micro-CT imaging is indeed a very popular non-destructive method, notably in paleontology, as it allows for high-quality images of internal structures (Skinner & Hung, 1989; Goodman & Rose, 1990; Marchewka *et al*., 2014). It relies on X-ray computed microtomography of the specimen through hundreds of radiographies taken from different angles and transformed into virtual slices. Thus, depending on the resolution, µCT scanning may allow

for results similar to those of histology without damaging the specimen and with infinite virtual slicing possibilities. A pioneering comparison between µCT scan and microscopy for hypoplasia investigation even pointed out that the former method i) had better results in detecting the defects and ii) provided more accurate measurements than microscopy (Marchewka *et al*., 2014).

In this paper, we propose to test the reliability of µCT scan in hypoplasia detection and to weigh the costs and benefits of using micro-CT imaging to study enamel hypoplasia on fossil rhinocerotoid teeth. We also investigate the potential of µCT scan to detect hidden defects on *Cadurcotherium* teeth with cement obscuring partly or totally their enamel surface.

MATERIALS AND METHODS

Our dataset is composed of two groups of rhinocerotoid teeth. The first one, our control sample to test for the ability of µCT scan to properly detect hypoplasia defects, consisted of eight isolated cheek teeth (including one with no taxonomical identification), a maxilla bearing P2-P3, and three associated teeth (p4-m1-m2) all presenting hypoplasia, except for the associated m1, which is very worn. All teeth come from the locality of Béon 1 and belong to the rhinocerotids *Plesiaceratherium mirallesi, Prosantorhinus douvillei*, and Rhinocerotidae indet. (one tooth). Béon 1 is a late early Miocene locality from southwestern France (Montréal-du-Gers; MN4; ~ 17 Mya; Figure 1). It has yielded a species-rich vertebrate fauna with over 60 species identified of rodents, carnivores, proboscideans, perissodactyls, artiodactyls, birds, squamates, and amphibians (Crouzel *et al*., 1988; Antoine & Duranthon, 1997; Rage & Bailón, 2005) including five rhinocerotid species (Antoine, 2002). The site is reconstructed as an oxbow lake surrounded by open woodlands under subtropical climatic conditions. All the material from Béon 1 is stored at the Muséum de Toulouse (MHNT).

The second group consisted of 11 isolated teeth of the Oligocene amynodontid genus *Cadurcotherium* – four being assigned to *C. minum* and seven to *C. cayluxi* – all from the Phosphorites du Quercy, in SW France (Figure 1). Two specimens of *C. minum* originate from Pech Crabit (MP23, early Oligocene; Laudet *et al*., 1997). They are curated in the University of Montpellier collections (UM; France). All other specimens belong to the Léenhardt collection. Although they are not located or dated precisely, most of these specimens were already figured and/or measured in the seminal revision of *Cadurcotherium* by Roman & Joleaud (1909). This very collection was considered lost in the meantime (e.g., Ménouret, 2018), until its recent donation to the University of Montpellier through Jean-Pierre Aguilar. *Cadurcotherium* teeth are high crowned and further characterized by the presence of coronary cement that obscures partially or totally enamel surface. This subsample was used to test the potential of µCT scan and segmentation to detect hypoplasia when enamel is obscured

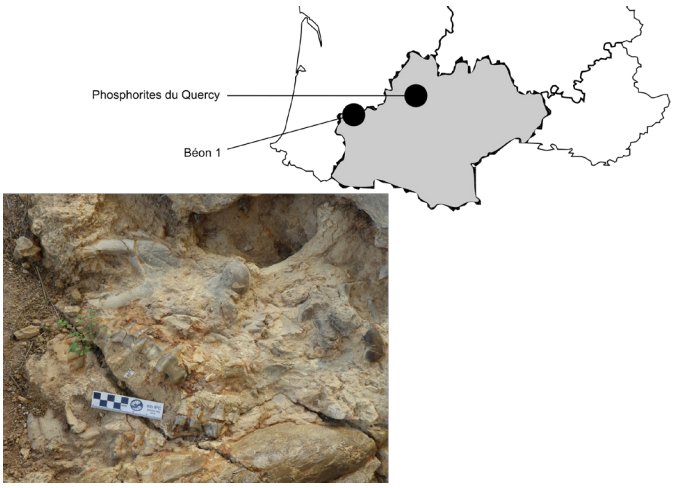

Figure 1. Localization of fossil localities of Béon 1 (late early Miocene) and Phosphorites du Quercy (Oligocene) that yielded the studied rhinocerotoid teeth. Photo illustrating an example of rhinocerotid remains found at Béon 1, Montréal-du-Gers (MN4; Southwestern France). Credit: Pierre-Olivier Antoine. Phosphorites du Quercy not illustrated as the exact provenance of most of the studied specimens is not known.

The micro-CT imaging was performed at the Institut des Sciences de l'Evolution de Montpellier (ISE-M), using the micro-CT Scanner EasyTom 150 kV from the Montpellier Ressources Imagerie (MRI) platform. We used a copper filter (0.3 mm) to limit beam hardening and the parameters were set to 130 kV, 230 µA (except for Béon 1 maxilla 2015/183: 224 µA), 360° of rotation, 10 frames averaging. The isometric voxel sizes resulting from these scans ranged between 23.8 and 56.6 µm. Corrections (geometric, automatic point correlation, ring artefacts, and beam correction) and reconstruction were done using Xact (v.2 revision 11025; 2019). Reconstructions were then studied using Fiji for ImageJ (v1.48) and AVIZO (2019.3). A supplementary step of segmentation was undertaken in AVIZO for specimens presenting cement (*Cadurcotherium* teeth).

Naked eye investigation consisted in detecting and identifying the defects based on the *Fédération Dentaire Internationale* Index (1982). Types of defects are illustrated in Figure 2. Pits were considered as one hypoplasia event and not scored individually in our counts. Measurements (distance to enamel-dentine junction, width of the defect) were taken using a caliper (Fischer Darex France, Ref PAL250 – Capacity: 200 mm, Precision: 0.02 mm).

We conducted statistics on our dataset to assess if hypoplasia detection was enhanced or not with µCT scan imaging. As our samples were restricted ($n < 15$), we chose the non-parametric Wilcoxon test, which compares the medians of two groups. We used the paired-sample version of this test due to the non-independence of the samples (same specimens observed with the naked eye and µCT scanned). Following the statement of the American Statistical Association (ASA) on p-values (Wasserstein & Lazar, 2016; Wasserstein *et al*., 2019), we deliberately avoided the use of the term "statistically significant" and the classical associated thresholds, but gave exact p-values instead.

RESULTS

The results of our analyses with naked eye and µCT scan are compared in Table 1 and all details are available in Supplementary S1. We found a noticeably greater median of detected defects with the µCT scan when both Béon 1 and *Cadurcotherium* specimens were considered ($V = 66.5$, p-value = 0.01643), and when *Cadurcotherium* specimens were considered alone ($V = 15$, p-value = 0.02724). However, the number of defects detected by the naked eye was not different from that using micro-CT imaging in the Béon sample when analyzed separately (control group; $V = 21.5$, p-value = 0.1171).

Béon 1 sample: control group

The rhinocerotid sample from Béon 1 was our positive control, as all 13 teeth from Béon 1 displayed hypoplasia except for the m1 from the associated p4-m2 that was too worn for hypoplasia investigation. All macroscopically-detected hypoplasias were retrieved on µCT scan reconstructions and selected virtual slices (Figures 3-4). Sometimes, several virtual slices had to be considered, as defects were found on different parts of the same tooth. For five teeth, additional defects were detected using µCT scan imaging (Table 1; Figure 3C, D, E; Figure 4D, E). In total, we detected 1.3 times more hypoplasias with the µCT scan than with naked eye.

Cadurcotherium sample: hypoplasia and cement

The *Cadurcotherium* sample (11 teeth) allowed for testing of the capacity of µCT scan to detect hypoplasias on teeth covered by cement. While only one hypoplasia could be seen with naked eye, the use of the µCT scan revealed 10 supplementary defects on five specimens (Table 1; Figures 5-6). Despite

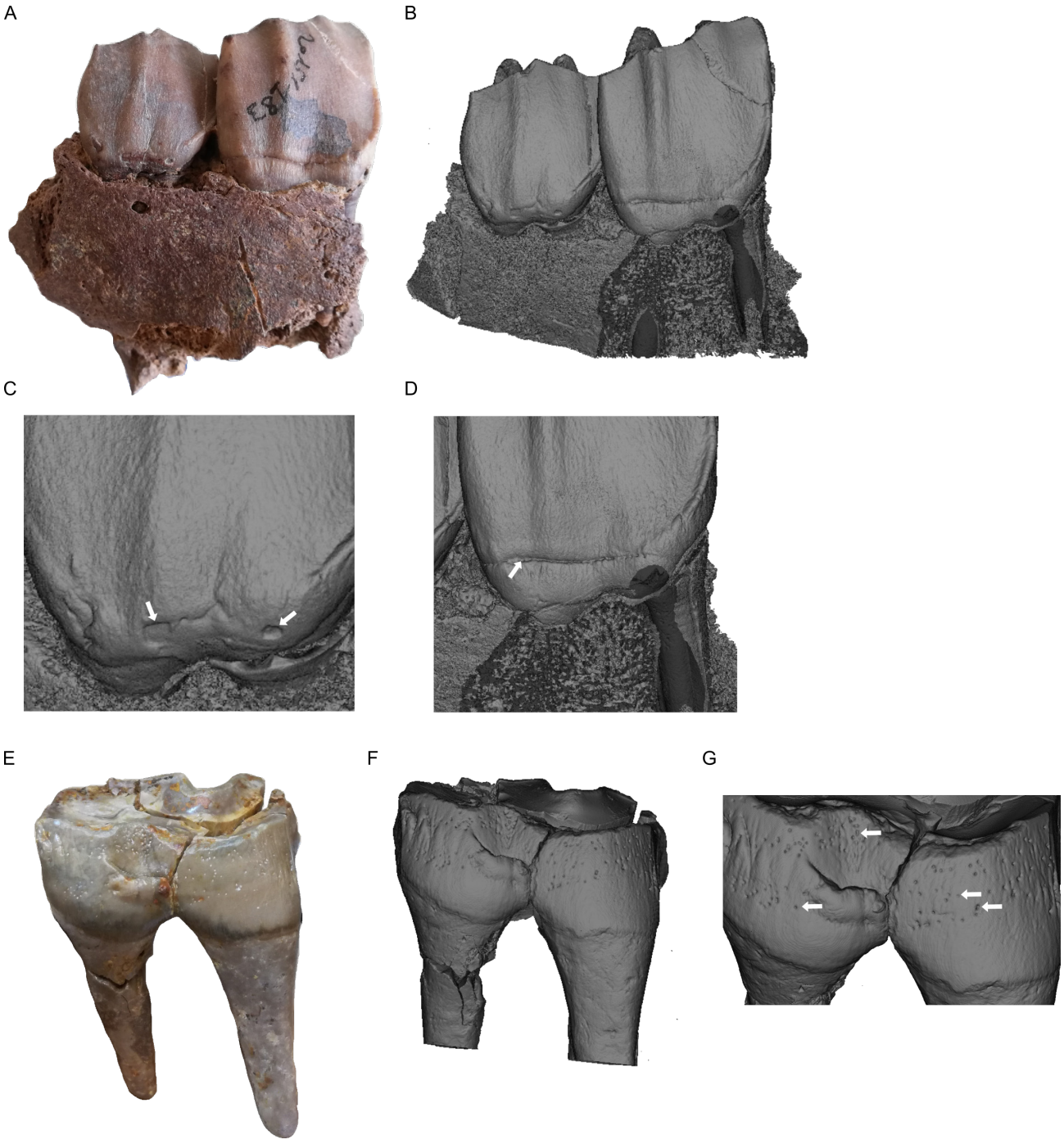

Figure 2. The three different types of enamel hypoplasia considered in this study illustrated on pictures and 3D reconstructions of Béon 1 specimens. 2015-183 specimen, right maxilla of *Prosantorhinus douvillei* with P2 and P3 bearing aplasias and LEH respectively: **A.** Photo in labial view, **B.** 3D reconstruction in labial view, **C.** Zoom on P2 aplasias indicated by white arrows, **D.** Zoom on P3 LEH indicated by white arrow. Béon 2003 F1 17 specimen, left p4 of *Plesiaceratherium mirallesi* displaying multiple pits: **E.** Photo in labial view, **F.** 3D reconstruction in labial view, **G.** Zoom on the zone displaying multiple pits, four of which are pointed by white arrows. Not to scale.

such greater detection, six teeth - out of the ten not displaying macroscopical hypoplasia – still did not present hypoplasia at the microscopic scale. The virtual slices also showed surprising features of enamel microstructure, such as folds for the CF24 specimen (Figure 6C).

DISCUSSION

Our results, although on a restricted sample of rhinocerotoid teeth, confirmed that µCT scan is a reliable approach to study hypoplasia, as previously stated (Marchewka *et al*., 2014; Xing *et al*., 2016). Indeed, all macroscopically-spotted defects were retrieved on 3D reconstructions and selected virtual slices (Table 1; Figures 3 to 6). Moreover, our results suggest that µCT scan investigation has the potential to reveal more hypoplastic defects than naked eye inspection. Contrary to the naked eye approach, we were able to measure width and depth of the defects more precisely and on more defects on the virtual slices (Supplementary S1). These measurements might be crucial to some studies, as width of the defect is associated with its duration, and depth with its severity (Skinner &

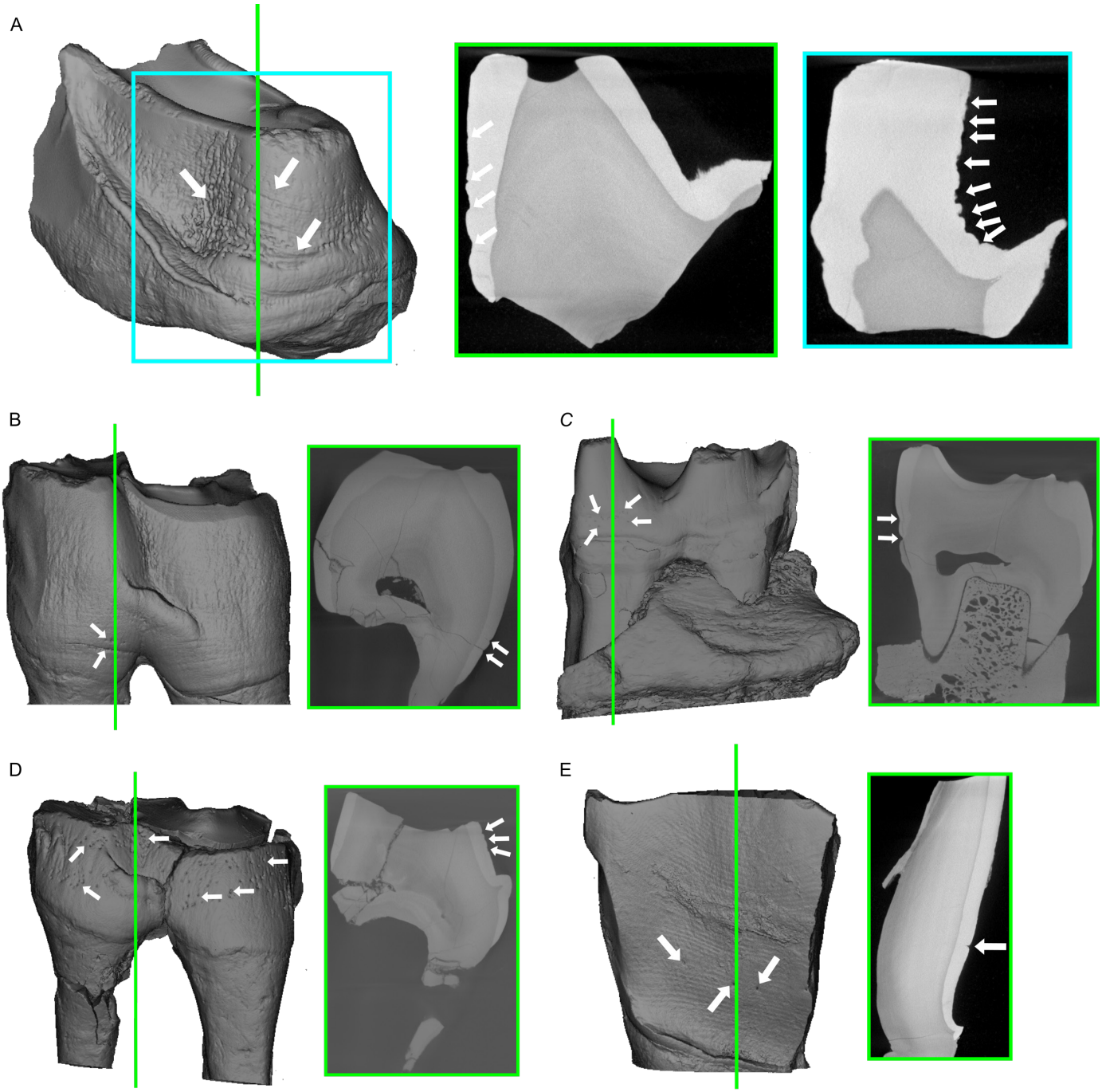

Figure 3. 3D reconstructions and virtual slices of Béon 1 *Plesiaceratherium mirallesi* and Rhinocerotidae indet. teeth with hypoplasia defects highlighted. Virtual slices correspond to the plan indicated by green or blue lines (approximate position) and white arrows indicate hypoplasia events. 3D reconstructions and associated virtual slices of *Pl. mirallesi* specimens: **A.** Béon 267 lingual view of the protoloph of a M1-2 with LEHs and pits, **B.** Béon E2 18 labial view of a left p4 (associated with Béon E2 11) with LEH and pit, **C.** Béon E2 11 lingual view of a left m2 (associated with Béon E2 18) with LEH and pits, **D.** Béon 2003 F1 17 labial view of a left p4 with multiple pits; and Rhinocerotidae indet specimen: **E.** Béon 1993 labial view of the ectoloph of a left cheek tooth.

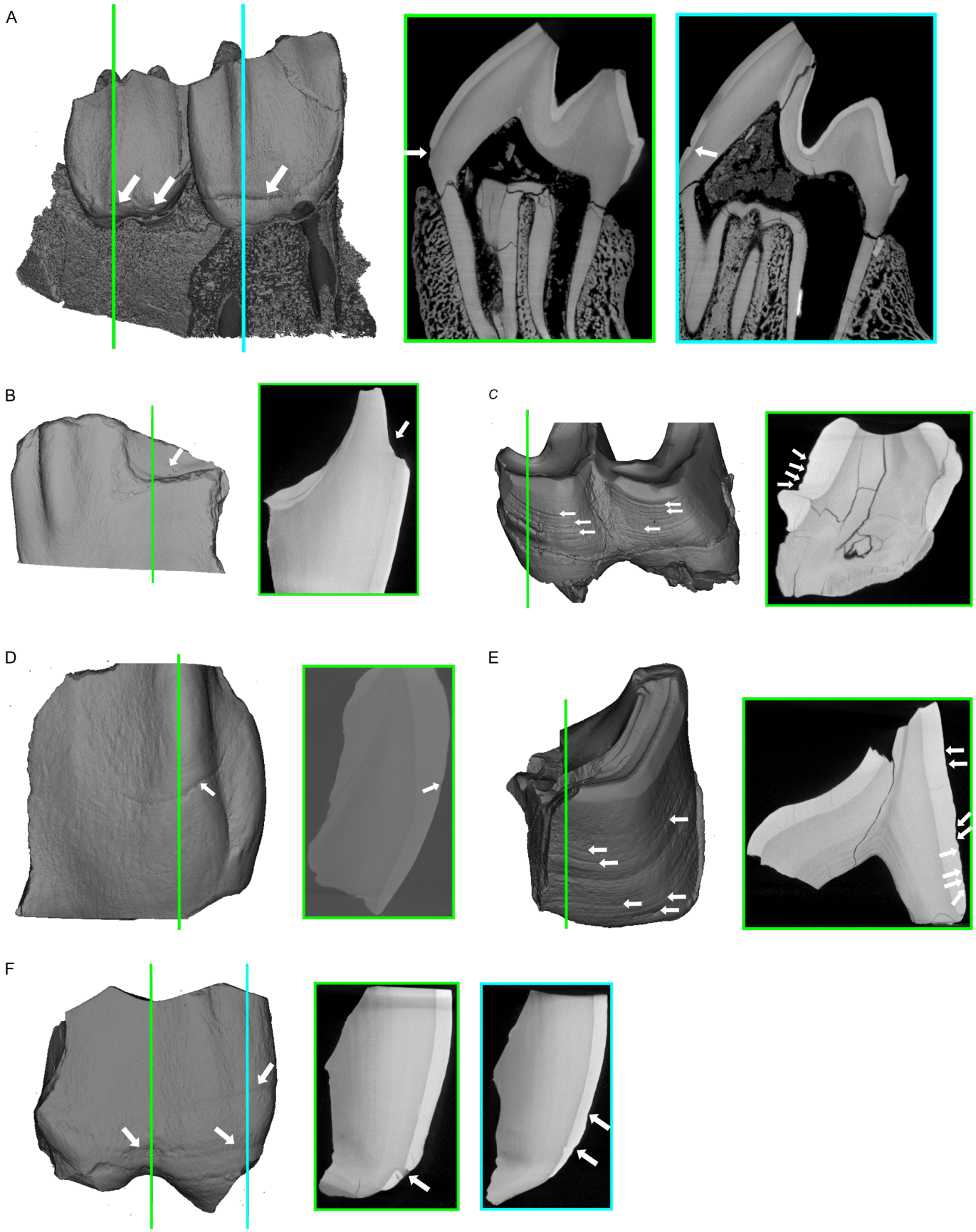

Figure 4. 3D reconstructions and virtual slices of Béon 1 *Prosantorhinus douvillei* teeth with hypoplasia defects highlighted. Virtual slices correspond to the plan indicated by green or blue lines (approximate position) and white arrows indicate hypoplasia events. 3D reconstructions and associated virtual slices of *Pr. douvillei* specimens: **A.** 2015-183 labial view of right P2 and P3 on a maxilla displaying aplasias and a LEH respectively, **B.** Béon 9 labial view of the ectoloph of a right M1-2 with aplasia, **C.** Béon 2003 SN 10 labial view of a left m3 with multiple LEHs, **D.** Montréal 1987 labial view of the ectoloph of a left M1-2 with a LEH, **E.** Béon SN73 labio-distal view of the hypoloph of a left m1-2 with multiple LEHs, **F.** Béon 1998 F1 2090 labial view of the ectoloph of a left P3? with LEHs and pits.

Table 1. Comparison of enamel hypoplasia detection with naked eye or CT scan on rhinocerotoid teeth from Béon 1 (late early Miocene; France) and Phosphorites du Quercy (Oligocene; France). To avoid confusion in the genera, *Plesiaceratherium mirallesi* is abbreviated as *Pl. mirallesi* and *Prosantorhinus douvillei* as *Pr. douvillei*. LEH stands for linear enamel hypoplasia and defect for uncategorized hypoplasia. Lowercases stand for lower teeth and upper cases stand for upper teeth. P/p: premolar and M/m: molar. Wear according to the stages proposed by Hillman-Smith et al. (1986).

Storage	Locality	Specimen	Species	Tooth	Position	Side	Wear	Naked eye	CT-scan
MHNT	Béon 1	2015-183	*Pr. douvillei*	Maxillary					
				P2	Upper	Right	5	2 aplasias	2 defects
				P3	Upper	Right	5	LEH	1 defect
MHNT	Béon 1	Montréal 1987	*Pr. douvillei*	M1-2	Upper	Left	6	LEH	4 defects
MHNT	Béon 1	Béon SN73	*Pr. douvillei*	m1-2	Lower	Left	5	4 LEHs Accentuated lines	8 LEHs
MHNT	Béon 1	Béon 1998 F1 2090	*Pr. douvillei*	P3?	Upper	Left	6/7	2 LEHs	2 defects
MHNT	Béon 1	Béon 9	*Pr. douvillei*	M1-2	Upper	Right	6	Aplasia	1 defect
MHNT	Béon 1	Béon 2003 SN 10	*Pr. douvillei*	m3	Lower	Left	6/7	8 LEHs	4 LEHs
MHNT	Béon 1		*Pl. mirallesi*	Associated					
		Béon 2002 E2 18		p4	Lower	Left	7	2 defects: LEH and some pits	2 defects: LEH and pit
		Béon 2002 E2 30		m1	Lower	Left	8	/	/
		Béon 2002 E2 11		m2	Lower	Left	6	Pits	2 defects: LEH and pits
MHNT	Béon 1	Béon 267	*Pl. mirallesi*	M1-2	Upper	Left	6	4 LEHs Pits	2 major defects 5 minor defects
MHNT	Béon 1	Béon 2003 F1 17	*Pl. mirallesi*	p4	Lower	Left	7	Pits	4 defects
MHNT	Béon 1	Béon 1993	Rhinocerotidae indet	Cheek tooth	Upper	Left	6	Thinner enamel	2 defects
UM	Phosphorites du Quercy	UM-ACQ-1531	*C. cayluxi*	m2	Lower	Left	6	LEH	3 LEHs
UM	Phosphorites du Quercy	UM-ACQ-1533	*C. cayluxi*	p4	Lower	Right	5	/	/
UM	Phosphorites du Quercy	CF.24	*C. cayluxi*	M1	Upper	Right	5	/	/
UM	Phosphorites du Quercy	CF.25	*C. cayluxi*	M1	Upper	Left	6	/	/
UM	Phosphorites du Quercy	FL.2	*C. cayluxi*	M1	Upper	Left	6	/	/
UM	Phosphorites du Quercy	FL.10	*C. cayluxi*	m3	Lower	Left	6	/	2 LEHs
UM	Phosphorites du Quercy	FL.11	*C. cayluxi*	m2	Lower	Right	8	/	3 LEHs and pits
UM	Phosphorites du Quercy	FL.13	*C. minum*	m1	Lower	Left	8	/	/
UM	Phosphorites du Quercy	/	*C. minum*	M1	Upper	Left	6	/	Vertical hypoplasias
UM	Pech Crabit (MP23; Lot, France)	UM-PCT-1102	*C. minum*	m3	Lower	Left	2/3	/	2 slight LEHs
UM	Pech Crabit (MP23; Lot, France)	UM-PCT-1105	*C. minum*	P2	Upper	Right	5	/	/

Hung, 1989; Skinner & Goodman, 1992; McGrath *et al*., 2018, 2021). Unfortunately, little is known about the timing of dental development in rhinoceros, which makes correlation to a precise age or duration impossible.

Previous studies interested in the microscopical detection (optic, SEM, confocal or µCT scan) of hypoplasia defects found similar results, with more defects and abnormalities spotted with these approaches than with the naked eye (Hassett, 2014; Marchewka *et al*., 2014). These differences between macro- and micro-observations are less marked on cheek teeth (premolars and molars), at least in hominoids, maybe because only more major defects appear clearly on posterior teeth due to the very acute striae of Retzius angles especially in hominoids molar teeth, leading to relatively shallower defects on the tooth surface (McGrath, *pers. comm.*, 2021). This greater detection is however constrained by the resolution of the µCT imaging

(here with a voxel size of ~24-57 µm), and might still miss minor defects (e.g., shallow defects in fast growing species ; McGrath *et al*., 2021). Hassett (2014) also pointed out all the limits of microscopic approaches, as these methods are time-consuming, expensive, and they require specific analytical tools, despite noting that they might become cheaper and more accessible in the future and supplant naked eye. In this respect, µCT scan investigation might not be as pertinent as previously stated (Table 2).

For unobscured teeth (Béon 1 sample; positive control), we did not detect any noticeable differences in the number of defects recorded between the two methods. Moreover, we suspect that some defects detected on virtual slices might not really be hypoplasia, highlighting the over-detection risk at the microscopic scale mentioned above (Hassett, 2014). In fact, as no threshold to differentiate "normal" from pathological enamel has been defined (Upex & Dobney, 2012; McGrath *et al*., 2018, 2021), some observed features might only be natural variations of the enamel thickness. Indeed, enamel deposition is not a continuous nor constant process, and natural stops occur periodically during amelogenesis leaving traces on the enamel. This is for instance the case of cross-striations (daily features) and Retzius lines (Tafforeau *et al*., 2007; O'Hara & Guatelli-Steinberg, 2020). These "irregularities" at the enamel surface might be confusingly interpreted as hypoplasia defects although they might be normal variations of the amelogenesis or "coronal waisting" (Skinner *et al*., 2012). Besides this issue, the identification of the defect (LEH, pit, aplasia) is rarely evident on virtual slices alone, and must be assessed either on the physical specimen (naked eye) or on its 3D reconstruction.

Table 2. Comparison of micro-CT scan and naked eye methods for detecting enamel hypoplasia. Cost range is given for local researchers and is based on the rates proposed by several micro-tomography platforms in France (MRI Montpellier, AniRA-ImmOs Lyon, AST-RX Paris). Scanning time is given for isolated rhinocerotoid teeth.

	CT-scan	Naked eye
Precision	Very good Possibility to measure width and depth of the defects	Good Width imprecise and depth not measurable
Cost	~ 125 to 250 € / half day But up to 600 € / acquisition	None
Time (per tooth)	20min scan > 30min treatment	< 5min / tooth
Sample size	Limited due to time and cost Possibility to include germs within bone, unprepared teeth, teeth with cement Physical size limitation (depending on the chamber of the CT-scan)	Limited to availability
Detection	Depending on resolution	Under-detection risk

Concerning *Cadurcotherium* teeth, for which enamel surface was hidden partly or totally by cement, micro-CT imaging proved useful. Indeed, without µCT scan investigation, these specimens would have been excluded from hypoplasia investigation. For species displaying thick cement cover on their teeth (e.g., derived elasmotheriines or equines among perissodactyls; Antoine, 2002), this can be a critical issue as

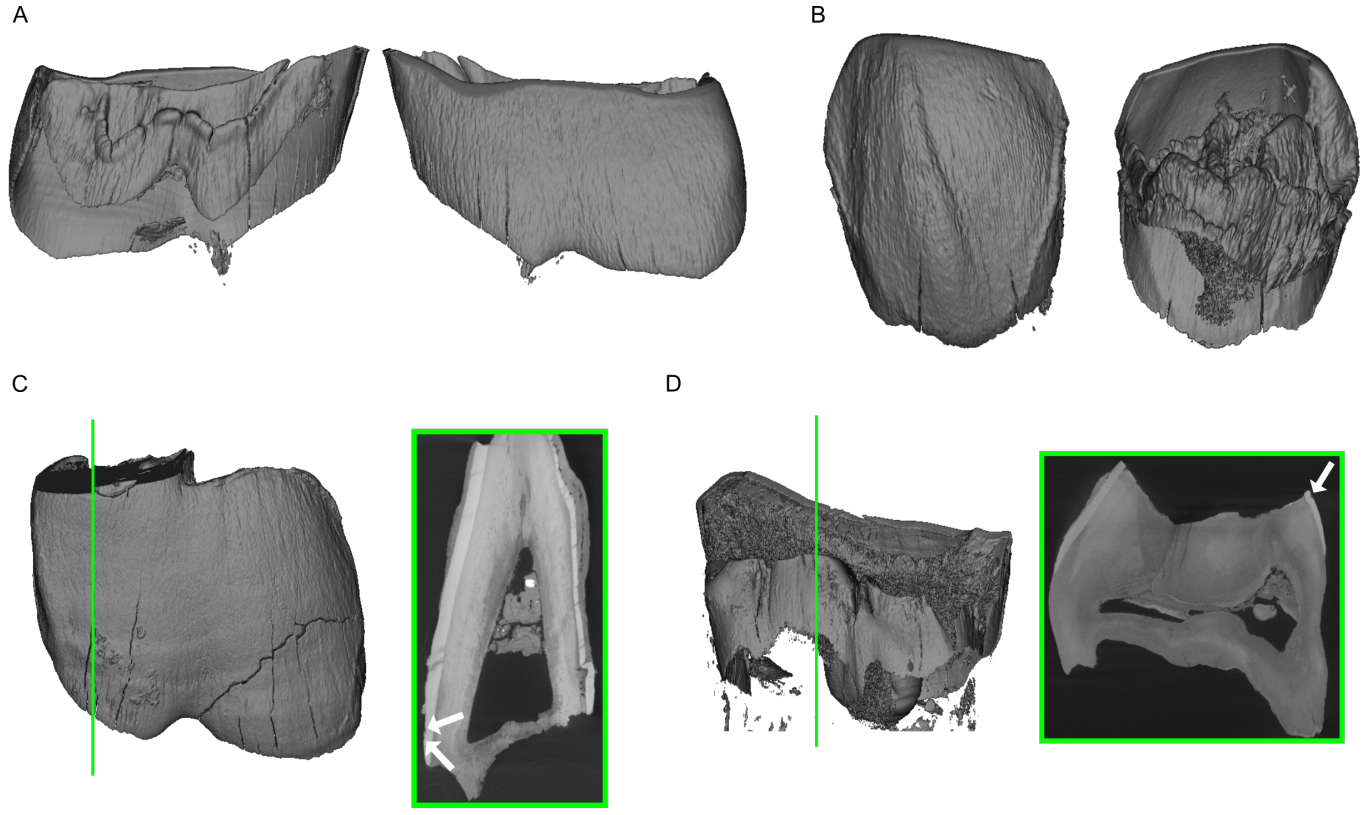

Figure 5. 3D reconstructions and virtual slices of *Cadurcotherium minum* teeth from Phosphorites du Quercy (Oligocene, France) with hypoplasia defects highlighted. Virtual slices correspond to the plan indicated by green or blue lines (approximate position) and white arrows indicate hypoplasia events. 3D reconstructions of specimen: **A.** FL.13 m1 left in lingual view (left) and labial view (right), and **B.** PCT 1105 P2 right in labial view (left) and lingual view (right). 3D reconstructions and associated virtual slices of specimen: **C.** PCT 1102 m3 left with two LEHs, **D.** No number M1 left with vertical hypoplasias.

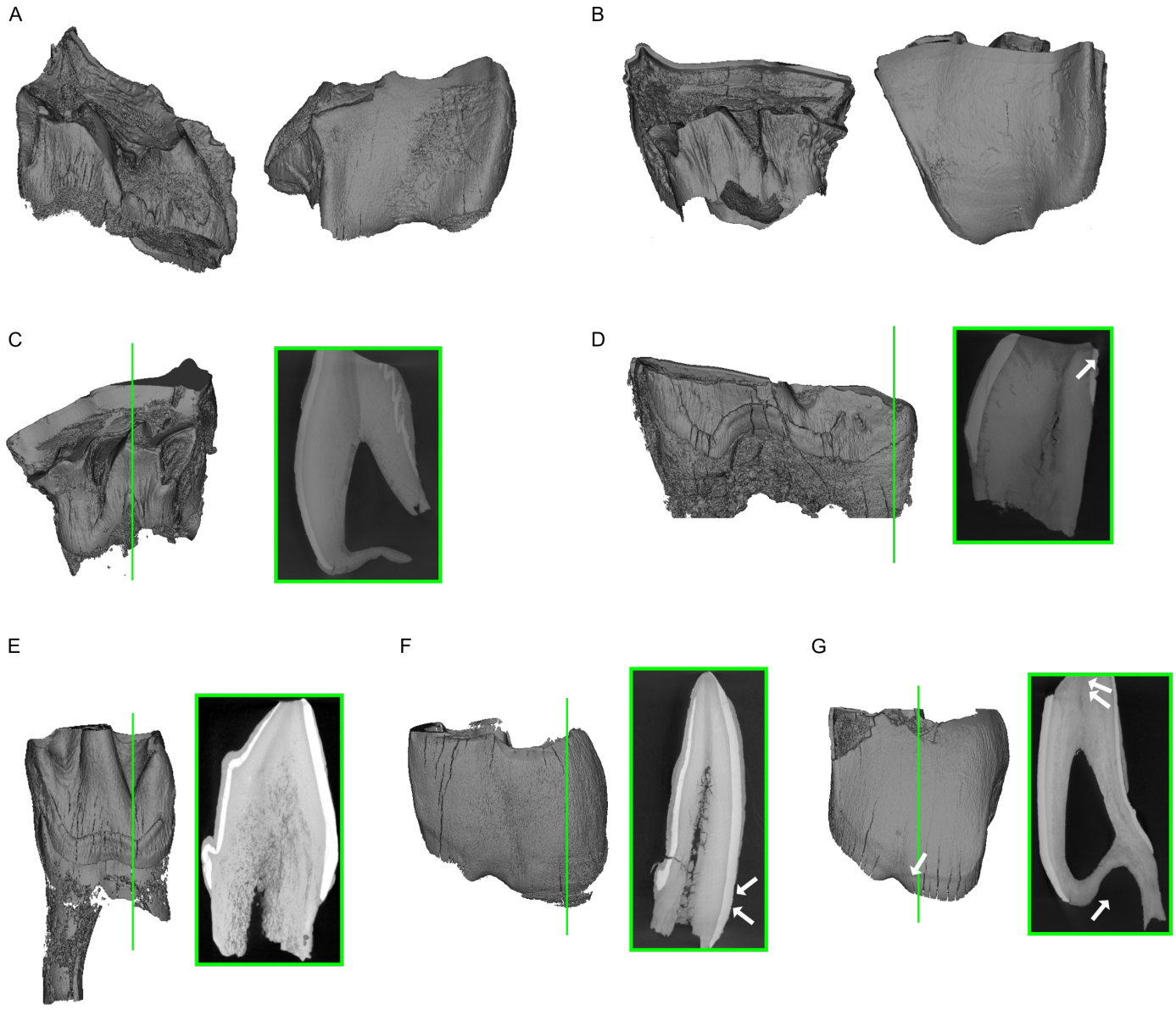

Figure 6. 3D reconstructions and virtual slices of *Cadurcotherium cayluxi* teeth from Phosphorites du Quercy (Oligocene, France) with hypoplasia defects highlighted. Virtual slices correspond to the plan indicated by green or blue lines (approximate position) and white arrows indicate hypoplasia events. 3D reconstructions of specimen: **A.** CF.25 M1 left in lingual view (left) and labial view (right) and **B.** FL.2 M1 left in labial view (left) and lingual view (right). 3D reconstructions and associated virtual slices of specimen: **C.** CF.24 M1 right with strange enamel microstructure, **D.** FL.11 m2 right with 3 LEHs and pits observed on various virtual slices, **E.** ACQ-1533 p4 right with strange enamel microstructure, **F.** FL.10 m3 left with 2 LEHs visible on virtual slice, and **G.** ACQ-1531 m3 left with a mascrocopical LEH and 3 LEHs identified on virtual slice.

sample size might be drastically reduced without the use of the µCT scan (Table 2). For this kind of teeth, micro-CT imaging and segmentation might be really helpful allowing to take into account teeth presenting cement, obscured by sediment, or included in bone (e.g., germs) in hypoplasia studies.

CONCLUSIONS

Using µCT scan has allowed for detecting additional hypoplasia defects compared to naked eye identification on *Cadurcotherium* cheek teeth, widely covered by coronary cement. Conversely, no critical differences between naked eye and µCT scan were found for our control sample, hence not justifying the systematic use of µCT scan for hypoplasia investigation. Thus, we would recommend the use of µCT scan on restricted samples or on specific specimens only (e.g., teeth obscured by cement, sediment, or unerupted), because of the cost and time needed for such approach.

ACKNOWLEDGMENTS

This research has been partly funded by the foundation Yves Coppens (excavation at Béon 1) and by a “Bourse de Mobilité Doctorale” granted by the Association Française des Femmes Diplômées des Universités. We are indebted to Yves Laurent and Pierre Dalous (MHNT), and to Anne-Lise Charruault (UM) for providing the specimens from the collections they are/were responsible of. We are grateful to Renaud Lebrun and the MRI platform, member of the national infrastructure France-BioImaging supported by the French National Research

Agency (ANR-10-INBS-04, «Investments for the future»), the labex CEMEB (ANR-10-LABX-0004) and NUMEV (ANR-10-LABX-0020), for granting access to the µCT scanner. This manuscript has benefited from considerable improvements, thanks to the constructive remarks of Kate McGrath and of an anonymous reviewer.

BIBLIOGRAPHY

Antoine, P.-O., 2002. Phylogénie et évolution des Elasmotheriina (Mammalia, Rhinocerotidae). Mémoires du Muséum National d'Histoire Naturelle, 188:1-359.

Antoine, P.-O., Duranthon, F., 1997. Découverte de *Protaceratherium minutum* (Mammalia, Rhinocerotidae) dans le gisement Orléanien (MN 4) de Montréal-du-Gers (Gers). Annales de Paléontologie (Vert.-Invert.), 83:201-213.

Bacon, A.-M., Antoine, P.-O., Nguyen, T. M. H., Westaway, K., Zhao, J., Nguyen, A. T., Duringer, P., Ponche, J.-L., Sam, C. D., Truong, H. N., Tran, T. M., Nguyen, T. K. T., Pham, T. S., Demeter, S., 2020. Linear enamel hypoplasia in large-bodied mammals of Pleistocene northern Vietnam, with a special focus on *Pongo*. Quaternary International. https://doi.org/10.1016/j.quaint.2020.07.013

Bacon, A.-M., Antoine, P.-O., Huong, N. T. M., Westaway, K., Tuan, N. A., Duringer, P., Zhao, J., Ponche, J.-L., Dung, S. C., Nghia, T. H., Minh, T. T., Son, P. T., Boyon, M., Thuy, N. T. K., Blin, A., Demeter, F., 2018. A rhinocerotid-dominated megafauna at the MIS6-5 transition: The late Middle Pleistocene Coc Muoi assemblage, Lang Son province, Vietnam. Quaternary Science Reviews, 186:123-141. https://doi.org/10.1016/j.quascirev.2018.02.017

Barrón-Ortiz, C. I., Jass, C. N., Barrón-Corvera, R., Austen, J., Theodor, J. M., 2019. Enamel hypoplasia and dental wear of North American late Pleistocene horses and bison: an assessment of nutritionally based extinction models. Paleobiology, 45:484-515. https://doi.org/10.1017/pab.2019.17

Bratlund, B., 1999. Taubach revisited. Jahrbuch Des Römisch-Germanischen Zentralmuseums Mainz, 46:61-174.

Cabec, A. L., Tang, N., Tafforeau, P., 2015. Accessing developmental information of fossil hominin teeth using new synchrotron microtomography-based visualization techniques of dental surfaces and interfaces. PLOS ONE, 10:e0123019. https://doi.org/10.1371/journal.pone.0123019

Chollet, M. B., Teaford, M. F., 2010. Ecological stress and linear enamel hypoplasia in *Cebus*. American Journal of Physical Anthropology, 142:1-6. https://doi.org/10.1002/ajpa.21182

Crouzel, F., Duranthon, F., Ginsburg, F., 1988. Découverte d'un riche gisement à petits et grands mammifères d'âge Orléanien dans le département du Gers (France). Comptes Rendus de l'Académie des Sciences. Série 2, Mécanique, Physique, Chimie, Sciences de l'univers, Sciences de La Terre, 307:101-104.

Dobney, K., Ervynck, A., 1998. A protocol for recording linear enamel hypoplasia on archaeological pig teeth. International Journal of Osteoarchaeology, 8:263-273. https://doi.org/10.1002/(SICI)1099-1212(199807/08)8:4<263::AID-OA427>3.0.CO;2-P

Dobney, K., Ervynck, A., 2000. Interpreting developmental stress in archaeological pigs: the chronology of linear enamel hypoplasia. Journal of Archaeological Science, 27:597-607. https://doi.org/10.1006/jasc.1999.0477

Ensor, B. E., Irish, J. D., 1995. Hypoplastic area method for analyzing dental enamel hypoplasia. American Journal of Physical Anthropology, 98:507-517. https://doi.org/10.1002/ajpa.1330980410

Fédération Dentaire Internationale, 1982. An epidemiological index of development defects of dental enamel (DDE index). International Dental Journal, 42:411-426.

Fourvel, J.-B., Fosse, P., Fernandez, P., Antoine, P. O., 2015. Large mammals of Fouvent-Saint-Andoche (Haute-Saône, France): a glimpse into a Late Pleistocene hyena den. Geodiversitas, 37:237-266. https://doi.org/10.5252/g2015n2a5

Franco, K. M. D., Line, S. R. P., de Moura-Ribeiro, M. V. L., 2007. Prenatal and neonatal variables associated with enamel hypoplasia in deciduous teeth in low birth weight preterm infants. Journal of Applied Oral Science, 15:518-523. https://doi.org/10.1590/S1678-77572007000600012

Franz-Odendaal, T., Chinsamy, A., Lee-Thorp, J. A., 2004. High prevalence of enamel hypoplasia in an early Pliocene giraffid (*Sivatherium hendeyi*) from South Africa. Journal of Vertebrate Paleontology, 24:235-244. https://doi.org/10.1671/19

Franz-Odendaal, T. A., Lee-Thorp, J. A., Chinsamy, A., 2003. Insights from stable light isotopes on enamel defects and weaning in Pliocene herbivores. Journal of Biosciences, 28:765-773. https://doi.org/10.1007/BF02708437

Goodman, A. H., Rose J. C., 1990. Assessment of systemic physiological perturbations from dental enamel hypoplasias and associated histological structures. American Journal of Physical Anthropology, 33:59-110. https://doi.org/10.1002/ajpa.1330330506

Goodman, A. H., Rose J. C., 1991. Dental enamel hypoplasias as indicators of nutritional status. In: Kelley M. A., Larsen C. S. (Eds.), Advances in Dental Anthropology, Wiley-Liss, New-York, pp. 279-293.

Guatelli-Steinberg, D., 2001. What can developmental defects of enamel reveal about physiological stress in nonhuman primates? Evolutionary Anthropology: Issues, News, and Reviews, 10:138-151. https://doi.org/10.1002/evan.1027

Hassett, B. R., 2014. Missing defects? A comparison of microscopic and macroscopic approaches to identifying linear enamel hypoplasia. American Journal of Physical Anthropology, 153:463-472. https://doi.org/10.1002/ajpa.22445

Henriquez, A. C., Oxenham, M. F., 2017. An alternative objective microscopic method for the identification of linear enamel hypoplasia (LEH) in the absence of visible perikymata. Journal of Archaeological Science: Reports, 14:76-84. https://doi.org/10.1016/j.jasrep.2017.05.040

Hillman-Smith, A. K. K., Owen-Smith, N. R., Anderson, J. L., Hall-Martin, A. J., Selaladi, J. P., 1986. Age estimation of the white rhinoceros (*Ceratotherium simum*). Journal of Zoology, 210:355-377. https://doi.org/10.1111/j.1469-7998.1986.tb03639.x

Kierdorf, H., Witzel, C., Upex, B., Dobney, K., Kierdorf, U., 2012. Enamel hypoplasia in molars of sheep and goats, and its relationship to the pattern of tooth crown growth. Journal of Anatomy, 220:484-495. https://doi.org/10.1111/j.1469-7580.2012.01482.x

Laudet, F., Denys, C., Fernández-Jalvo, Y., 1997. Taphonomie des vertébrés oligocènes de Pech Crabit (Lot, Phosphorites du Quercy): Implications géodynamiques et paléoécologiques des remaniements post-mortem. Geobios, 30:307-313. https://doi.org/10.1016/S0016-6995(97)80036-8

Lukacs, J. R., 1999. Enamel hypoplasia in deciduous teeth of great apes: Do differences in defect prevalence imply differential levels of physiological stress? American Journal of Physical Anthropology, 110:351-363. https://doi.org/10.1002/(SICI)1096-8644(199911)110:3<351::AID-AJPA7>3.0.CO;2-2

Marchewka, J., Skrzat, J., Wrobel, A., 2014. Analysis of the enamel hypoplasia using micro-CT scanner versus classical method. Anthropologischer Anzeiger, 71:391-402. https://doi.org/10.1127/0003-5548/2014/0366

McGrath, K., El-Zaatari, S., Guatelli-Steinberg, D., Stanton, M. A., Reid, D. J., Stoinski, T. S., Cranfield, M. R., Mudakikwa, A., McFarlin, S. C., 2018. Quantifying linear enamel hypoplasia in Virunga Mountain gorillas and other great apes. American Journal of Physical Anthropology, 166:337-352. https://doi.org/10.1002/ajpa.23436

McGrath, K., Limmer, L. S., Lockey, A.-L., Guatelli-Steinberg, D., Reid, D. J., Witzel, C., Bocaege, E., McFarlin, S. C., El Zaatari,

S., 2021. 3D enamel profilometry reveals faster growth but similar stress severity in Neanderthal versus *Homo sapiens* teeth. Scientific Reports, 11:522. https://doi.org/10.1038/s41598-020-80148-w

Mead, A. J., 1999. Enamel hypoplasia in Miocene rhinoceroses (*Teleoceras*) from Nebraska: evidence of severe physiological stress. Journal of Vertebrate Paleontology, 19:391-397. https://doi.org/10.1080/02724634.1999.10011150

Ménouret, B., 2018. Le genre *Cadurcotherium* (Rhinocerotoidea) en Europe ; synthèse des connaissances et révision systématique. Revue de Paléobiologie, Genève, 37:495-517.

Neiburger, E. J., 1990. Enamel hypoplasias: Poor indicators of dietary stress. American Journal of Physical Anthropology, 82:231-232. https://doi.org/10.1002/ajpa.1330820211

Niven, L. B., Egeland, C. P., Todd, L. C., 2004. An inter-site comparison of enamel hypoplasia in bison: implications for paleoecology and modeling Late Plains Archaic subsistence. Journal of Archaeological Science, 31:1783-1794. https://doi.org/10.1016/j.jas.2004.06.001

Ogilvie, M. D., Curran, B. K., Trinkaus, E., 1989. Incidence and patterning of dental enamel hypoplasia among the Neandertals. American Journal of Physical Anthropology, 79:25-41. https://doi.org/10.1002/ajpa.1330790104

O'Hara, M. C., Guatelli-Steinberg, D., 2020. Differences in enamel defect expression and enamel growth variables in *Macaca fascicularis* and *Trachypithecus cristatus* from Sabah, Borneo. Journal of Archaeological Science, 114:105078. https://doi.org/10.1016/j.jas.2020.105078

Rage, J.-C., Bailón, S., 2005. Amphibians and squamate reptiles from the late early Miocene (MN 4) of Béon 1 (Montréal-du-Gers, southwestern France). Geodiversitas, 27:413-441.

Roman, F., Joleaud, L., 1909. "*Cadurcotherium*" de l'Isle-sur-Sorgue (Vaucluse) et révision du genre "*Cadurcotherium*." Archives du Muséum d'Histoire naturelle de Lyon, 10:1-44. https://doi.org/10.3406/mhnly.1909.963

Rose, J. C., 1977. Defective enamel histology of prehistoric teeth from illinois. American Journal of Physical Anthropology, 46:439-446. https://doi.org/10.1002/ajpa.1330460309

Rothschild, B. M., Martin, L. D., Lev, G., Bercovier, H., Bar-Gal, G. K., Greenblatt, C., Donoghue, H., Spigelman, M., Brittain, D., 2001. *Mycobacterium tuberculosis* complex DNA from an extinct bison dated 17,000 years before the Present. Clinical Infectious Diseases, 33:305-311. https://doi.org/10.1086/321886

Sabel, N., Klingberg, G., Dietz, W., Nietzsche, S., Norén, J. G., 2010. Polarized light and scanning electron microscopic investigation of enamel hypoplasia in primary teeth. International Journal of Paediatric Dentistry, 20:31-36. https://doi.org/10.1111/j.1365-263X.2009.01006.x

Skinner, M., Goodman, A. H., 1992. Anthropological uses of developmental defects of enamel. Skeletal Biology of Past Peoples: Research Methods, 153-174.

Skinner, M. F., Hung, J. T. W., 1989. Social and biological correlates of localized enamel hypoplasia of the human deciduous canine tooth. American Journal of Physical Anthropology, 79:159-175. https://doi.org/10.1002/ajpa.1330790204

Skinner, M. F., Pruetz, J. D., 2012. Reconstruction of periodicity of repetitive linear enamel hypoplasia from perikymata counts on imbricational enamel among dry-adapted chimpanzees (*Pan troglodytes verus*) from Fongoli, Senegal. American Journal of Physical Anthropology, 149:468-482. https://doi.org/10.1002/ajpa.22145

Skinner, M. F., Skinner, M. M., Boesch, C., 2012. Developmental defects of the dental crown in chimpanzees from the Taï National Park, Côte d'Ivoire: coronal waisting. American Journal of Physical Anthropology, 149:272-282. https://doi.org/10.1002/ajpa.22123

Small, B. W., Murray, J. J., 1978. Enamel opacities: prevalence, classifications and aetiological considerations. Journal of Dentistry, 6:33-42. https://doi.org/10.1016/0300-5712(78)90004-0

Tafforeau, P., Bentaleb, I., Jaeger, J.-J., Martin, C., 2007. Nature of laminations and mineralization in rhinoceros enamel using histology and X-ray synchrotron microtomography: potential implications for palaeoenvironmental isotopic studies. Palaeogeography, Palaeoclimatology, Palaeoecology, 246:206-227. https://doi.org/10.1016/j.palaeo.2006.10.001

Upex, B., Dobney, K., 2012. Dental enamel hypoplasia as indicators of seasonal environmental and physiological impacts in modern sheep populations: a model for interpreting the zooarchaeological record. Journal of Zoology, 287:259-268. https://doi.org/10.1111/j.1469-7998.2012.00912.x

Wasserstein, R. L., Lazar, N. A., 2016. The ASA statement on p-Values: Context, process, and purpose. The American Statistician, 70:129-133. https://doi.org/10.1080/00031305.2016.1154108

Wasserstein, R. L., Schirm, A. L., Lazar, N. A., 2019. Moving to a World Beyond "p < 0.05." The American Statistician, 73:1-19. https://doi.org/10.1080/00031305.2019.1583913

Windley, Z., Weller, R., Tremaine, W. H., Perkins, J. D., 2009. Two- and three-dimensional computed tomographic anatomy of the enamel, infundibulae and pulp of 126 equine cheek teeth. Part 2: Findings in teeth with macroscopic occlusal or computed tomographic lesions. Equine Veterinary Journal, 41:441-447. https://doi.org/10.2746/042516409X391033

Witzel, C., Kierdorf, U., Schultz, M., Kierdorf, H., 2008. Insights from the inside: histological analysis of abnormal enamel microstructure associated with hypoplastic enamel defects in human teeth. American Journal of Physical Anthropology, 136:400-414. https://doi.org/10.1002/ajpa.20822

Xing, S., Guatelli-Steinberg, D., O'Hara, M., Li, J., Wei, P., Liu, W., Wu, X., 2016. Micro-CT imaging and analysis of enamel defects on the Early Late Pleistocene Xujiayao juvenile. International Journal of Osteoarchaeology, 26:935-946. https://doi.org/10.1002/oa.2504